CHAPTER 47

ACTION OF NON-LINEAR WAVES AT A SOLID WALL

by

Mohamed S. Nasser[1], M.ASCE and John A. McCorquodale[2], AM.ASCE

ABSTRACT

A one-dimensional finite difference model is developed to simulate the action of long non-linear shallow water waves at a solid barrier. A damping parameter is introduced to account for the centrifugal effects in the incident wave. A stability criterion for $\Delta t/\Delta x$ is suggested. The numerical predictions of reflection and run-up compare satisfactorily with experimental results.

INTRODUCTION

The phenomenon of run-up and reflection resulting from water waves impinging on breakwaters is an important problem in coastal engineering. Breakwaters are designed to avoid excessive overtopping. On the other hand, reflection causes local disturbances that persist for some distance outside of the breakwater.

This paper presents a one-dimensional, finite difference model simulating wave motion in front of a vertical, solid breakwater. The discretization of the solution domain is constrained

---

[1]Assistant Professor, Department of Civil Engineering, Concordia University, SGW Campus, Montreal, Quebec, Canada.

[2]Professor, Department of Civil Engineering, University of Windsor, Windsor, Ontario, Canada.

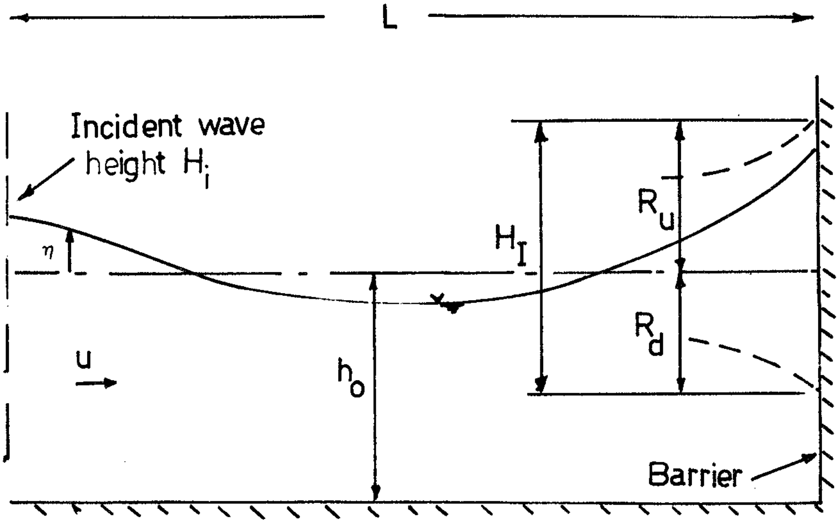

Fig. 1. Definition of Problem

by the characteristic directions to improve numerical convergence and stability. The model predicts wave run-up and rush-down on the breakwater as well as the reflection coefficient. Long, shallow, non-breaking waves are considered in the analysis, and the model is capable of treating both symmetric and asymmetric waves. The model should aid in designing vertical solid breakwaters and is being modified to accommodate sloping sections.

DEVELOPMENT OF MODEL

Figure 1 defines some of the variables of the study. Assuming long, shallow water waves, i.e., approximately hydrostatic pressure distribution, it can be shown that the governing equations of motion and continuity are, respectively (1, 4):

$$\frac{\partial u}{\partial t} + u \frac{\partial u}{\partial x} + g \frac{\partial \eta}{\partial x} = -gS_f \tag{1}$$

$$\frac{\partial \eta}{\partial t} + u \frac{\partial \eta}{\partial x} + (h_o+\eta) \frac{\partial u}{\partial x} = 0 \tag{2}$$

where u = horizontal velocity; η = perturbation height with respect to the still water level, h_o; g = acceleration of gravity; S_f = friction slope = $\frac{u|u|}{C_f(h_o+\eta)}$; C_f = Chezy friction factor; the bed is assumed horizontal.

Eq. 1 describes fairly accurately the motion of long linear waves. For non-linear, i.e., asymmetric waves, hydrodynamic pressure may become appreciable. However, in this study, Eqs. 1 and 2 are applied to asymmetric waves with an allowance for additional damping due to centrifugal effects. Assuming a sinusoidal wave (Fig. 2), the total head loss, h_t, between sections 1 and 2 may be expressed as

$$h_t = h_f + \varepsilon h_c \tag{3}$$

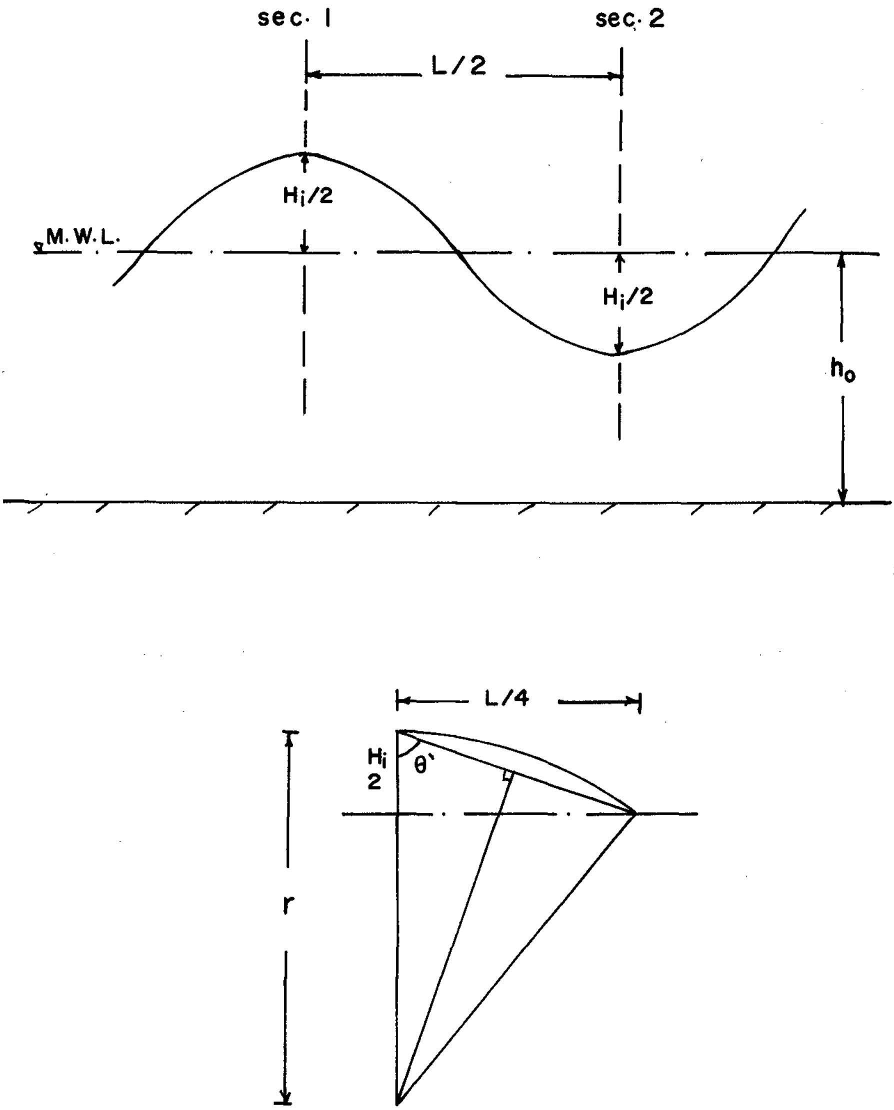

Fig. 2. Approximation of Centrifugal Effect

in which h_f = frictional head loss between sections 1 and 2; h_c = difference in centrifugal pressure head between the two sections; ε = empirical constant.

Applying Newton's second law to compute the approximate centrifugal pressure, it can be shown that h_c is given by (3)

$$h_c = \frac{2h_o}{gr} v^2 \tag{4}$$

where r = radius of curvature of water surface;
v = mean velocity in the vertical.

The frictional head loss, h_f, can be represented by

$$h_f = \frac{v^2 L}{2C_f^2 h_o} \tag{5}$$

in which L is the incident wave length.

Also, the total head loss, h_t, may be assumed as

$$h_t = \frac{v^2 L}{2C_t^2 h_o} \tag{6}$$

where C_t is the equivalent Chezy factor accounting for both frictional and centrifugal effects.

Substituting Eqs. 4 through 6 into 3 and rearranging, gives

$$C_t = \sqrt{\frac{gLrC_f^2}{gLr+4\varepsilon h_o^2 C_f^2}} \tag{7}$$

From Fig. 2, the value of r may be approximated as follows:

$$r \simeq [(Hi/2)^2 + (L/4)^2]/H_i \tag{8}$$

Based on a correlation with laboratory experiments, Eq. 7 takes the form

$$C_t = \sqrt{\frac{gLrC_f^2}{gLr+1.2h_o^2C_f^2}} \tag{9}$$

Since r varies inversely with wave steepness, S, Eq. 9 indicates the energy dissipation due to centrifugal action increases with wave steepness.

In order to proceed to the finite difference formulation, η is made dimensionally identical to u through the transformation

$$c = \sqrt{g(h_o+\eta)} \tag{10}$$

which represents a local wave celerity utilized as a measure of η.

The equations of motion and continuity, in terms of c, along with the total differentials of u and c constitute the hyperbolic system of equations governing the phenomenon as given by the matrix form (1):

$$\begin{bmatrix} 1 & u & 0 & 2c \\ 0 & c & 2 & 2u \\ dt & dx & 0 & 0 \\ 0 & 0 & dt & dx \end{bmatrix} \begin{Bmatrix} \frac{\partial u}{\partial t} \\ \frac{\partial u}{\partial x} \\ \frac{\partial c}{\partial t} \\ \frac{\partial c}{\partial x} \end{Bmatrix} = \begin{Bmatrix} -gS_f \\ 0 \\ du \\ dc \end{Bmatrix} \tag{11}$$

The above system yields the following positive and negative characteristic directions:

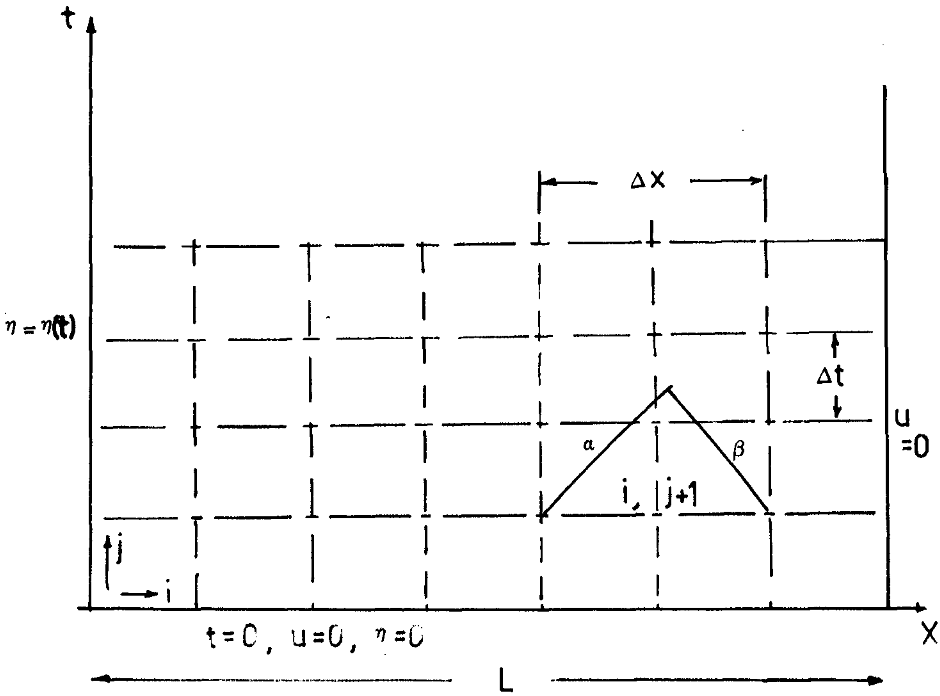

Fig. 3. Boundary Conditions and Discretization of the x-t Plane

$$\alpha = \frac{dx}{dt}\Big|_{+} = u + c \tag{12}$$

$$\beta = \frac{dx}{dt}\Big|_{-} = u - c \tag{13}$$

Based on these directions, the condition,

$$\frac{\Delta t}{\Delta x} \leq \frac{1}{2}\,(u+c)^{-1} \tag{14}$$

is obtained and used, initially, to control the finite difference, x-t plane (Fig. 3) for stability and convergence (5). The equations of motion and continuity, from Eq. 11, are discretized using central differences in space and forward differences in time, viz.

$$u(i,j+1) = u(i,j) - \frac{\Delta t}{\Delta x}\{u(i,j)[u(i+1,j)-u(i-1,j)] + 2c(i,j)[c(i+1,j)-c(i-1,j)] + g\Delta x S_f(i,j)\} \tag{15}$$

$$c(i,j+1) = c(i,j) - \frac{\Delta t}{\Delta x}\{u(i,j)[c(i+1,j)-c(i-1,j)] + [c(i,j)/2][u(i+1,j)-u(i-1,j)]\} \tag{16}$$

Eqs. 15 and 16 were used to advance the solution from initially still water conditions, i.e., $u = o$ and $c = \sqrt{gh_o}$. The boundary condition at the right end of the solution domain, is zero normal velocity at all times. The incident wave is originated in the model at one wave length away from the breakwater; this is the minimum distance required to ensure the generation of at least one loop and one node in the standing wave pattern. The boundary condition simulates the vertical displacement of the incident wave which is represented by a composite as shown in Fig. 4. The amplitudes, A_1 and A_2, and the periods, T_1 and T_2, are proportioned so that volume continuity is satisfied which leads to

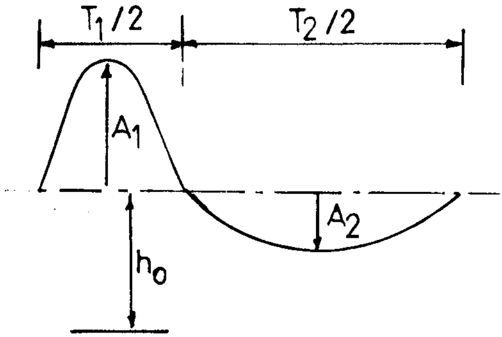

Fig. 4. Composite Input Wave

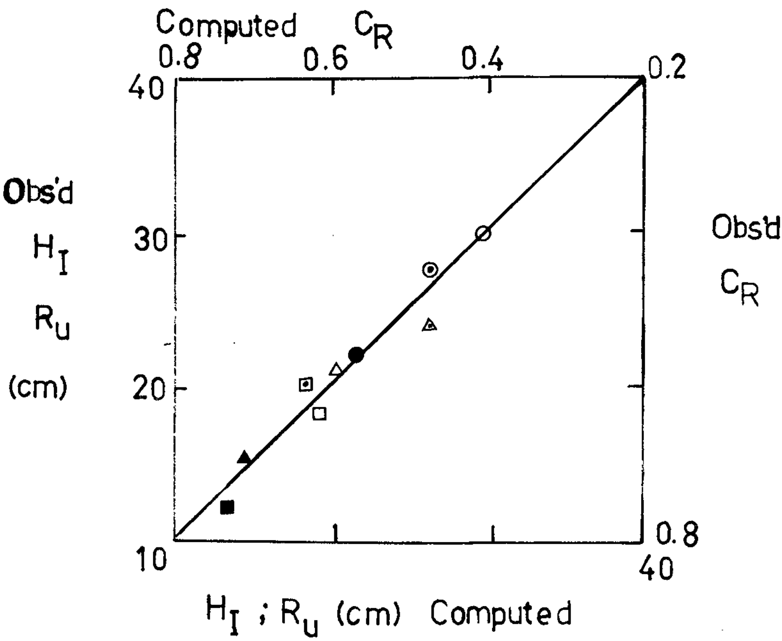

Fig. 5. Comparison of Observed and Predicted Values

$$A_1/A_2 = T_2/T_1 \tag{17}$$

In order to calculate the unknown dependent variable at each boundary, the value of the dependent variable specified by the boundary condition at time (j+1) was included in the calculation. This was achieved by combining the equations of motion and continuity, and discretizing the augmented equation by forward differences in space and time. Assuming that the boundary is located at the ith column, the unknown celerity at the breakwater is calculated by the α-characteristic difference equation,

$$\begin{aligned} c(i,j+1) = c(i,j) + 2\,\frac{\Delta t}{\Delta x}\,\{&c(i,j)u(i-1,j)/2 \\ &- c(i,j)[c(i,j)-c(i-1,j)]\} \end{aligned} \tag{18}$$

Likewise, a β-characteristic difference equation is used to find the unknown velocity at the left boundary, i.e.,

$$\begin{aligned} u(i,j+1) = u(i,j) &+ 2[c(i,j+1)-c(i,j)] + \\ \frac{2\Delta t}{\Delta x}\,\{&2[u(i,j)-c(i,j)][c(i+1,j)-c(i,j)] \\ &- [u(i,j)-c(i,j)][u(i+1,j)-u(i,j)] \\ &- \Delta x g S_f(i,j)u(i,j)/2\} \end{aligned} \tag{19}$$

Throughout the solution, the values of velocity, celerity and the non-linear friction term were improved, within each time increment, by an iterative procedure.

VERIFICATION OF MODEL

A laboratory investigation was conducted to evaluate the proposed mathematical model. The Test flume was 45.8 cm wide and 11 m long with plexiglass walls and aluminum bed. The slider-crank, wave machine used has adjustable stroke and speed that were selected to produce shallow water waves. The breakwater was simulated by a vertical plexiglass barrier, located at 9.2 m away from the intermediate position of the wave paddle. Wave experiments were performed within the following range of variables:

h_o (cm)	22 - 38
H_i (cm)	4 - 24
Wave Period, T (sec)	2 - 5.8

In the experimental procedure, the stroke and speed were set so as to minimize surface disturbances and secondary waves. The incident wave celerity, c, was determined, prior to the interference of reflection, using a stop watch to time the movement of a wave peak over different distances. The wave period, T, was taken as the average of the rotation time of a point marked on the flywheel of the wave machine. The product of the values of c and T yielded the wave length, L. After a few wave traverses, an asymmetric standing wave pattern was observed to develop and stabilize with nodes and loops forming, alternately, at almost every quarter wave length. The measured loop height, h_p, and node height, h_n, were used to find the "apparent" incident wave height, H_i, and the "apparent" reflected wave height, H_r, according to the linear wave theory, i.e.,

$$H_i = \frac{1}{2} (h_p + h_n) \tag{20}$$

$$H_r = \frac{1}{2} (h_p - h_n) \tag{21}$$

The "apparent" reflection coefficient, C_R, was defined as:

$$C_R = H_r/H_i \tag{22}$$

The maximum limits of run-up, R_u, and rush-down, R_d, bounding the impact wave height, H_I, at the breakwater were recorded. The experimental measurements are estimated to have been within an accuracy of about $\pm$ 2 cm.

When the mathematical model was operated, using the equality condition in Eq. 14 with $u \simeq c \simeq \sqrt{gh_o}$, the procedure was numerically unstable. This instability is thought to originate from the boundary conditions, especially the incident wave boundary condition. The development of Eq. 14 does not consider this type of boundary condition. In order to obtain stability, it was necessary to reduce the time step to between 1/5 and 1/10 of limiting value in Eq. 14.

The stable model was run for the equivalent of 5 wave periods and the third, fourth and fifth periods were used to obtain average values for h_p, h_n, R_u, R_d and H_I. The apparent values of H_i and H_r were calculated from Eqs. 20 and 21, respectively. It is noted that the non-linear values of C_R are much less than for linear waves.

An attempt to make a third order Stokes correction to both experimental and numerical reflection coefficients was unsuccessful because most of the waves had high H_i/h_o and low h_o/L. Similarly, second or third order Stokes waves were not suitable to describe the observed incident waves. Fifth or higher order Stokes waves or cnoidal waves can be used with the model but more computation time would be required. The crests and troughs of the composite incident waves can be established using information presented by Bretschneider (2).

In Fig. 5 some experimental values of R_u, H_I and C_R are compared with those predicted by the model.

CONCLUSIONS

The simplified numerical model gives representation values for wave reflection and run-up at a solid barrier under attack by long non-linear shallow water waves. Numerical stability was achieved by reducing the method of characteristic time step to about 1/10 of its limiting value. An empirical damping parameter is introduced to account for centrifugal effects in the non-linear waves.

ACKNOWLEDGMENT

This research was supported, in part, by the National Research Council of Canada.

REFERENCES

1. Abbott, M.B., "An Introduction to the Method of Characteristics", American Elsevier Co., New York, 1966.

2. Bretschneider, C.L., "Selection of Design Waves for Offshore Structures", Trans. ASCE, Paper No. 3026, 1960.

3. Chow, V.T., "Open-channel Hydraulics", McGraw-Hill Co., New York, 1959.

4. Henderson, F.M., "Open Channel Flow", The Macmillan Co., New York, 1966.

5. Smith, C.D., "Numerical Solution of Partial Differential Equations", Oxford University Press, London, 1965.